EurJIC European Journal of Inorganic Chemistry
ChemPubSoc Europe
FULL PAPER

DOI:10.1002/ejic.201400052

Cyclometalated Complexes of Platinum(II) with 2-Vinylpyridine

Antonio Zucca,*[a] Luca Maidich,[a] Veronica Carta,[a] Giacomo L. Petretto,[a] Sergio Stoccoro,[a] Maria Agostina Cinellu,[a] Maria I. Pilo,[a] and Guy J. Clarkson[b]

Keywords: Metallacycles / Metalation / C–H activation / Platinum / Vinylidene ligands

The electron-rich platinum(II) derivatives $[Pt(R)_2(DMSO)_2]$ (R = Me, Ph) react with 2-vinylpyridine (L) to give the cyclometalated complexes [Pt(L–H)(R)(DMSO)] through C–H bond activation. Cyclometalation also occurs with [Pt(Me)(Cl)$(DMSO)_2$]. From the starting compounds, a series of cyclometalated complexes was obtained and characterised by analytical and spectroscopic methods. The molecular structures of [Pt(L–H)(Me)(PPh_3)] and [Pt(L–H)(Ph)(PCy_3)] were solved by X-ray diffraction analysis, and the results unambiguously demonstrate cyclometalation of 2-vinylpyridine. The five-membered cyclometalated ring is particularly stable, likely due to partial electronic delocalisation.

Introduction

Cyclometalation is a widely studied reaction[1] and the synthesis of new cyclometalated complexes continues to attract interest due to their promising applications in many fields.[2] In this context, five-membered cyclometalated platinum(II) complexes containing a C,N backbone have been extensively studied due to their cytotoxicity and luminescence properties.[3] Cyclometalated Pt^{II} complexes have also been studied as sensors, switches, and catalysts.[4] In addition, cyclometalation is also widely studied as an intramolecular analogue of intermolecular C–H bond activation.[1b,5] One of the most studied pro-ligands in this field is 2-phenylpyridine, the five-membered cyclometalated complexes of which have been the subject of a considerable number of papers.[6] Despite this, 2-vinylpyridine, a ligand that is able to give a similar five-membered cyclometalated ring with the same sequence of $C(sp^2)$ atoms, has been the subject of a relatively limited number of studies involving Pd,[7] Pt,[6a,8] Co,[9] Rh,[10] Ir,[11] Ru,[12] Os,[12d–13] platinum(II) derivatives *cis*-$[Pt(R)_2(DMSO)_2]$ (R = Me, Ph) and *trans*-[Pt(Me)(Cl)$(DMSO)_2$].

Results and Discussion

The electron-rich Pt^{II} complex *cis*-$[Pt(Me)_2(DMSO)_2]$ is a well-known cyclometalating precursor that is able to activate C–H bonds under mild conditions with methane evolution.[19] In the case of 2-vinylpyridine as L, reaction with *cis*-$[Pt(Me)_2(DMSO)_2]$ follows different routes depending on the reaction conditions. Under mild conditions, i.e., in acetone at room temperature, only displacement of one DMSO ligand by L occurs, to give the corresponding adduct *cis*-$[Pt(Me)_2(L)(DMSO)]$ (**1**), whereas under harsher conditions, such as in toluene at 80 °C, activation of a vinylic C–H bond occurs to give the cyclometalated species [Pt(L–H)(Me)(DMSO)] (**2**), with loss of methane (Scheme 1).

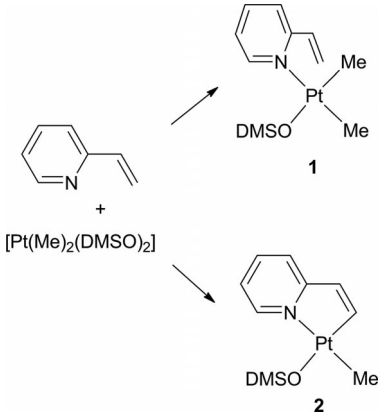

Scheme 1.

Adduct **1**, which is likely to be an intermediate species in the synthesis of **2**, was characterised by ^1H NMR spectroscopy. In particular, coordination of nitrogen was dem-

[a] Dipartimento di Chimica e Farmacia, Università degli Studi di Sassari,
Via Vienna 2, 07100 Sassari, Italy
E-mail: zucca@uniss.it
http://dcf.uniss.it/ws.php?mod=staff&usrid=257&page=itext&tag=curriculum&lang=en
[b] Department of Chemistry, University of Warwick,
CV4 7AL Coventry, United Kingdom
Supporting information for this article is available on the WWW under http://dx.doi.org/10.1002/ejic.201400052.

onstrated by the downfield shift of the H-6 proton and, mostly, by its coupling with the ^{195}Pt nucleus (δ = 8.83 ppm, $^{3}J_{Pt,H}$ = 20 Hz). Two methyl groups (δ = 0.47 ppm, $^{2}J_{Pt,H}$ = 89 Hz; 0.33 ppm, $^{2}J_{Pt,H}$ = 79 Hz) and a DMSO (δ = 2.79 ppm, $J_{Pt,H}$ = 14 Hz) complete the coordination around the metal. The coupling of the DMSO hydrogen atoms with the ^{195}Pt nucleus is very small, confirming a *trans* DMSO-Pt-Me arrangement. The signal of the Hα vinylic proton is strongly deshielded and coupled with platinum (δ = 8.21 ppm, $J_{Pt,H}$ = 10 Hz), with both factors suggesting an anagostic interaction[20] with the metal centre.

When rotation of the pyridine ligand around the Pt–N bond is restricted, the DMSO methyl groups should be diastereotopic; however, they appear instead in the ^{1}H NMR spectrum as a singlet with satellites, suggesting free rotation of the pyridine on the NMR time-scale. The NOESY spectrum of complex **1** is in line with this observation, showing no NOE contacts between pyridine protons and the other ligands, as may be expected in the case of free rotation. Furthermore, the NOESY spectrum showed clear cross-peaks between the three olefinic protons, as well as between the methyl group at δ = 0.48 ppm and the DMSO hydrogen atoms at δ = 2.90 ppm, allowing the assignment of Pt-bonded methyl signals. The methyl signal at δ = 0.33 ppm appears shifted to lower frequency, likely due to the shielding effect of the adjacent pyridine ring (Scheme 2).

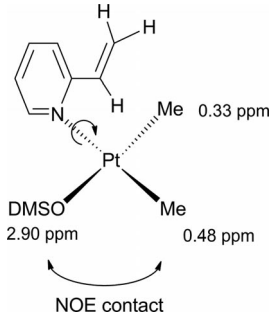

Scheme 2. Complex **1** with selected NMR spectroscopic data.

The progress of the metalation was investigated by ^{1}H NMR spectroscopic analysis at room temperature and at 40 °C. After addition of 2-vinylpyridine to [Pt(Me)$_2$(DMSO)$_2$] (0.05 M solution) rapid formation of the adduct **1** was observed in both cases, but complete conversion of [Pt(Me)$_2$(DMSO)$_2$] into the adduct **1** was slow, requiring more than one day at 40 °C, even in the presence of a slight excess of ligand. At 40 °C, conversion of the adduct **1** into the metalated complex **2** was observed; a conclusion that was supported by the appearance of methane in the spectrum at δ = 0.17 ppm. The concentration of **1** reached a maximum after approximately 30 minutes, then decreased as the concentration of **2** increased. After 3 h, [Pt(Me)$_2$(DMSO)$_2$], **1** and **2** are present in an approximate 2:1.5:1 molar ratio. Conversion of **1** into **2** also occurred at room temperature, but this was extremely slow. On the whole, the progress of the reaction was typical of a two-step consecutive reaction, as previously reported for other cyclometalation reactions involving [Pt(Me)$_2$(DMSO)$_2$].[19]

The reaction, however, was not clean, and other secondary species were present in solution. In toluene heated to reflux the conversion occurred with high yield, allowing the isolation of **2** in the solid state and its characterization by means of analytical and spectroscopic methods. In particular, the ^{1}H NMR spectrum clearly showed the absence of one olefinic proton and an AX system with satellites for the remaining two hydrogen atoms of the substituent. Pt–H coupling constants for these protons were particularly high, $^{2}J_{Pt,H}$ = 171 Hz for Hβ (δ = 7.42 ppm) and $^{3}J_{Pt,H}$ = 108 Hz for Hα (δ = 6.94 ppm). As a comparison, the analogous protons in the cationic complex [Pt(N,N)(L–H)]$^{+}$ [N,N being ArN=C(Me)–C(Me)=NAr] have ^{195}Pt–^{1}H coupling constants of 89 and 82 Hz for Hβ and Hα, respectively.[8]

The coordinated methyl (δ = 0.69 ppm, $^{2}J_{Pt,H}$ = 82.5 Hz) and DMSO (δ = 3.07 ppm, $^{3}J_{Pt,H}$ = 17 Hz) groups showed signals that were consistent with a Me *trans* to a nitrogen and a DMSO *trans* to a carbon, respectively. Coordination of the nitrogen was demonstrated by the shift of the H-6 signal and by its coupling to platinum (δ = 9.24 ppm, $^{3}J_{Pt,H}$ = 12 Hz), which was consistent with a *trans* N–Pt–CH$_3$ arrangement. The coordination geometry was confirmed by a 1D-NOE spectrum, which showed contacts of the coordinated methyl with the Hβ proton and the DMSO group (Scheme 3).

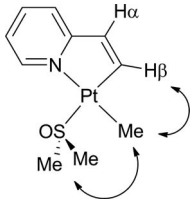

Scheme 3. Complex **2**: NOE contacts supporting the proposed geometry.

Further data for the characterisation was provided by ^{13}C NMR spectroscopic analysis, which showed two metalated carbon atoms: the methyl group, at –19.9 ppm, and the olefinic carbon, at δ = 163.2 ppm, both being coupled to platinum ($^{1}J_{Pt,C}$ = 756 and 1035 Hz, respectively). The coordination sphere is completed by DMSO (δ_C(DMSO) = 43.5 ppm, $^{2}J_{Pt,C}$ = 40 Hz) and pyridine [δ(C^6) 150.5 ppm, $^{2}J_{Pt,C}$ = 116 Hz]. It should be noted that the metalated olefinic carbon was strongly deshielded (δ = 163.2 ppm) with respect to the free ligand (δ = 118.1 ppm, $\Delta\delta$ = 45.1 ppm).

When *cis*-[Pt(Ph)$_2$(DMSO)$_2$] was used in place of *cis*-[Pt(Me)$_2$(DMSO)$_2$] the corresponding cyclometalated complex [Pt(L–H)(Ph)(DMSO)] (**3**) could be isolated with high yields and characterised. The ^{1}H NMR spectrum of **3** was similar to that of **2**, with some differences: five additional aromatic protons, two of which strongly coupled to platinum (H$_{ortho}$: δ = 7.39 ppm, $^{3}J_{Pt–H}$ = 71 Hz), demonstrate that a phenyl group is still coordinated to platinum. In this

case, also the absence of one olefinic proton accounts for C–H bond activation, and the remaining two signals demonstrate cyclometalation (Hβ: δ = 7.38 ppm, d with sat, $^2J_{Pt,H}$ = 180 Hz; Hα: δ = 6.90 ppm, d with sat, $^3J_{Pt,H}$ = 117 Hz). The DMSO resonates at low frequency compared to **2** (δ = 2.89 vs. 3.07 ppm in **2**) likely due to the shielding effect of the adjacent phenyl ring, which is probably nearly perpendicular to the square planar plane. The H-6 proton is also deshielded (δ = 9.29 ppm) and coupled with platinum, with the ^{195}Pt–^{1}H coupling constant (12 Hz) being very small, as for **2**, due to the strong *trans*-influence of the C(sp^2) phenyl carbon atom.

Cyclometalation of 2-vinylpyridine can be compared to that of 2-phenylpyridine (Phpy), which reacts easier, giving the corresponding five-membered cycloplatinated complexes [Pt(Phpy-H)(Me)(DMSO)] even at room temperature (^{1}H NMR proof).

Activation of a vinylic C–H bond also occurs with the less electron-rich complex *trans*-[Pt(Me)(Cl)(DMSO)$_2$] to give, in toluene at 80 °C, the cyclometalated complex [Pt(L–H)(Cl)(DMSO)] (**4**), also in this case with loss of methane. In complex **4** the DMSO ligand is coordinated *trans* to the nitrogen, instead of to the carbon; this is shown by the ^{195}Pt–^{1}H coupling constant value of the DMSO hydrogen atoms ($^3J_{Pt,H}$ = 26 Hz), which are typical of DMSO coordinated *trans* to a nitrogen atom. In this case, the pattern of the two remaining olefinic protons in the ^{1}H NMR spectrum also confirms metalation. These protons give rise to an AX system (δ = 6.65 ppm, $^2J_{Pt,H}$ = 97 Hz, Hα; δ = 7.26 ppm, $^3J_{Pt–H}$ = 84 Hz, Hβ). It is worth noting that in the electron poorer complex **4** the coupling constants between the olefinic protons and the platinum are smaller than the corresponding constants in the electron-rich species **2** and **3**. In particular, $^2J_{Pt,H}$ is almost halved in **4**. The H-6 proton is shifted to low fields and coupled to ^{195}Pt (δ = 9.10 ppm, $^2J_{Pt,H}$ = 35 Hz). Complex **4** was also obtained from **2** by reaction with HCl in acetone. The cyclometalated ring in complexes **2** and **4** is extremely stable; reaction of complex **2** with **1** or 2 equiv. of HCl only results in Pt-CH$_3$ protonolysis, with complex **4** being formed as the only reaction product, even after prolonged reaction times.

The isolation of different geometric isomers in the corresponding methyl and chloride cyclometalated complexes [Pt(N,C)(Me)(DMSO)] and [Pt(N,C)(Cl)(DMSO)] is well-known[21] and is attributable to the stronger *trans*-influence of Me compared to Cl. When possible, the ligand with the stronger *trans*-influence coordinates *trans* to the ligand with the weaker *trans*-influence, this leads to a DMSO coordinated *trans* to metalated vinylic carbon in **2** and **3**, with DMSO *trans* to nitrogen in **4**. To verify this result, we performed DFT calculations on the two geometric isomers, **A** and **B**, of complexes **2**–**4**, depicted in Figure 1 with their respective relative ΔH values (in kJ mol^{-1}, ZPE corrected, in vacuo). Full optimisation without constraints at the PBE0/def2-SVP level gave data that were consistent with experimental results, showing that the more stable isomers for complexes **2**–**3** have the **A** geometry; the opposite was observed for complex **4**.

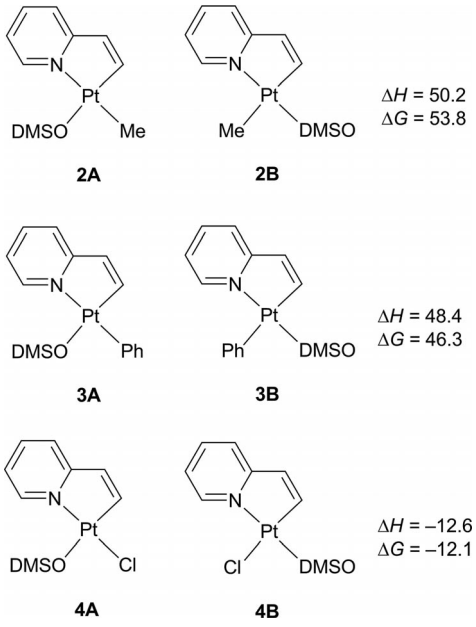

Figure 1. Isomers of complexes **2**–**4** and their relative stabilities. Values are DFT calculated differences in enthalpy (ΔH) and Gibbs free energy (ΔG) between the isomeric form **A** and **B** (298 K, kJ mol^{-1}, corrected for ZPE, in vacuo at PBE0/def2-SVP level of theory).

The effect of the stabilisation is predominantly enthalpic, as can be seen from the values in Figure 1, with less than 8% of the stabilisation energy being ascribable to the entropic contribution; these findings are consistent with previously reported data on analogous complexes.[22] Another interesting trend that is worth noting concerns the nature of the anionic ligand. Apparently, groups having a carbon donor, i.e., methyl and phenyl, lead to a larger difference in the energies between the **A** and **B** forms compared to the chloride. This result can be justified in terms of the *trans*-influence: for complexes **2**–**3** in form **B** a C-*trans*-C/S-*trans*-N arrangement is observed that is highly unstable (ca. 50 kJ mol^{-1}); on the other hand, in **4A** a S-*trans*-C/Cl-*trans*-N situation is found that is less unstable due to the smaller *trans* influence of the groups involved (ca. 12 kJ mol^{-1}). An analysis of the energy values permits the following *trans*-influence scale to be established: Me ≈ Ph > DMSO > Cl, which is perfectly consistent with the classic energy values.[23]

We also explored the potential energy surface (PES) associated with rotation of the DMSO ligand around the Pt–S bond in complexes **2**–**4** in both **A** and **B** forms (Figure 2). Analysis of the energy profiles obtained for form **A** did not indicate anything unusual, and the most stable conformations were always those with the oxygen of the DMSO pointing towards the H-6 of the pyridine. On the other hand, complexes of form **B** showed smaller activation energies for rotation around the Pt–S bond, which is reasonable considering the distance between the DMSO and the group of the cyclometalated ligand in the *cis* position.

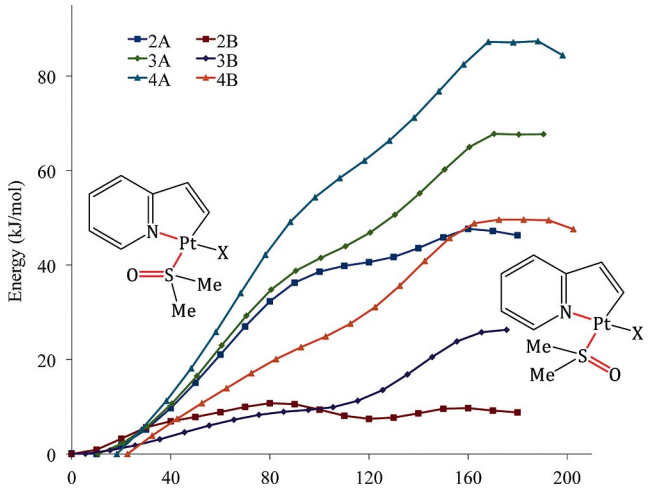

Figure 2. Potential energy surface calculated for rotation around the Pt–S bond in complexes **2**–**4** in forms **A** and **B** (VWN5/SBKJC level). Structures of form **A** are depicted to highlight the dihedral angle explored.

The finding that the most stable conformer of complexes of the type **A** has the oxygen of the DMSO close to H-6 is in agreement with its typical resonance in **2A** and **3A**.

A charge decomposition analysis (CDA)[24] was performed on complexes **2**–**4** to investigate the interaction energy of the DMSO with the remaining fragment of the complex. In all cases, the interaction energy was negative, with values ranging from –1.58 eV for **2** to –1.63 eV for **3** and –2.66 eV for **4**. Overall, however, the net charge donation is very similar in all three cases (ca. 0.27 e^-). A comparison between the interaction energies and the $^3J_{Pt,H}$ coupling constants for the protons of the DMSO show a reasonable qualitative agreement. We did not look for quantitative correlations between experiment and theory due to the required approximations involved in the calculations, but also because multiple bond coupling constants cannot be interpreted in a straightforward way because they are dependent on many different factors (i.e., angles, dihedrals, effects in space, etc.).

Substitution Reactions

DMSO is a good leaving group and, in complexes **2**–**4**, can be easily substituted by two-electron donor ligands to obtain a series of complexes with different electronic and steric properties. Substitution is particularly easy for complexes **2** and **3**, in which the DMSO is coordinated *trans* to a C(sp^2), a donor atom that has both high *trans* influence and *trans* effect. Reaction of **2** with PPh_3, PCy_3 or CO gives, under mild conditions, complexes [Pt(L–H)(Me)(PPh_3)] (**5**), [Pt(L–H)(Me)(PCy_3)] (**6**), and [Pt(L–H)(Me)(CO)] (**7**), respectively. Analogously, complexes [Pt(L–H)(Ph)(PPh_3)] (**8**) and [Pt(L–H)(Ph)(PCy_3)] (**9**), were obtained from **3**. Analytical and spectroscopic data for compounds **5**–**9** were consistent with the proposed formulations. In particular ^{31}P NMR spectra account for phosphanes being coordinated *trans* to a donor atom with high *trans*-influence, such as a C(sp^2) atom, as evidenced by the low value of the ^{195}Pt–^{31}P coupling constant (ca. 1800–2000 Hz; **5**: $J_{Pt,P}$ = 2020 Hz; **6**: $J_{Pt,P}$ = 1873 Hz; **8**: $J_{Pt,P}$ = 1990 Hz; **9**: $J_{Pt,P}$ = 1843 Hz); the coupling is stronger for PPh_3 (**5**, **8**) than for PCy_3 (**6**, **9**), and for Me-derivatives compared to Ph-derivatives. In species **5** and **6** the protons of the methyl groups appear as doublets with satellites, due to coupling both to ^{31}P and to ^{195}Pt (complex **5**: δ = 0.80 ppm, $^3J_{P,H}$ = 8.1, $^2J_{Pt,H}$ = 84 Hz; complex **6**: δ = 1.04 ppm, $^3J_{P,H}$ = 6.0, $^3J_{Pt,H}$ = 85 Hz), confirming the proximity of the CH_3 and PR_3 ligands. The geometry of complex **5** in solution was confirmed by a 1D-NOE experiment, which showed enhancement of signals at δ = 7.90 ppm (Hβ) and 7.79 (H*o* PPh_3) by irradiation of the methyl signal at δ = 0.80 ppm.

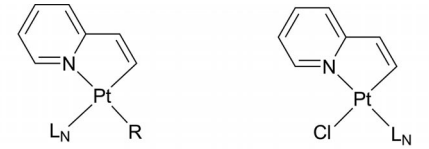

2, L_N = DMSO, R = Me
3, L_N = DMSO, R = Ph
5, L_N = PPh_3, R = Me
6, L_N = PCy_3, R = Me
7, L_N = CO, R = Me
8, L_N = PPh_3, R = Ph
9, L_N = PCy_3, R = Ph

4, L_N = DMSO
10, L_N = PPh_3

Complex [Pt(L–H)(Me)(CO)] (**7**), has a strong absorption in the IR spectrum at 2046 cm^{-1}, which is consistent with absorption bands found for analogous cyclometalated complexes (e.g., [Pt(bipy-H)(Me)(CO)] at 2044 cm^{-1}).[21] Interestingly, attempts to prepare the corresponding complex derived from 2-phenylpyridine, which should be similar in terms of electronic and steric properties, were not successful.[25] Complex **7** is stable in solution and in the solid state, even in the presence of water and air.

For chloride complex **4**, the coordinated DMSO *trans* to a nitrogen atom can be easily displaced by PPh_3 under mild conditions to give the corresponding phosphane complex [Pt(L–H)(Cl)(PPh_3)] (**10**), with high yields. Analytical and spectroscopic data are consistent with the proposed formulation, with a P–Pt–N *trans* arrangement, as indicated by the high $^1J_{Pt,P}$ value (4194 Hz). Due to the close proximity of the Cl ligand, the H-6 proton is strongly deshielded (δ = 9.45 ppm) with a coupling constant value ($^3J_{Pt-H}$ = 26.3 Hz) higher than that of complex **5**, due to the lower *trans* influence of PPh_3 with respect to Me. Coupling constants of the olefinic protons are smaller than in **5** ($J_{Pt,H}$ = 138.6 and 95.1 Hz for Hβ and Hα, respectively), and the signals are strongly shielded by the presence of PPh_3 in the *cis* position (δ = 6.39 ppm, Hβ, 6.63 ppm, Hα).

X-ray Structural Determinations

Crystals of **5** and **9** suitable for X-ray analysis were grown from acetone solutions. The crystal structures, shown in Figures 3 and 4, confirm the geometries predicted from NMR spectroscopy. The methyl and the phenyl ligands in

5 and **9**, respectively, are coordinated *trans* to the pyridine nitrogen, and the phosphane is coordinated *trans* to the cyclometalated carbon. In particular, crystals of **5** are composed of discrete molecules separated by van der Waals distances, in the monoclinic space group $P2_1/n$. The complex shows a remarkable planarity both in the coordination plane and in the cyclometalated moiety; the largest deviation from the best plane comprising the metal and its bounded atoms is for C108, which is 0.014 Å away from the plane.

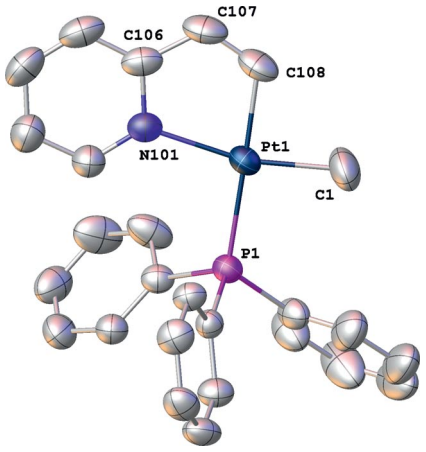

Figure 3. X-ray crystal structure of **5**. The thermal ellipsoids are drawn at 50% probability. Hydrogen atoms have been removed for clarity and only selected atoms are labelled. Selected bond lengths [Å] and angles [°]: Pt1–P1 2.3086(6); Pt1–N101 2.159(3); Pt1–C108 2.013(3); Pt1–C1 2.041(4); C107–C108 1.313(5); C106–C107 1.442(5); C106–N101 1.370(3); P1–Pt1–C1 92.7(1); C108–Pt1–C1 88.2(1); C108–Pt1–N101 78.1(1); N101–Pt1–P1 100.94(6); P1–Pt1–C108 178.51(9); N101–Pt1–C1 166.4(1).

Angles around platinum are in line with the steric requirements of the ligands. The cyclometalated ligand has a bite of 78.13(11)°, which is a low value that is consistent with those usually found for five-membered cyclometalates. As a comparison, the N–Pt–C angle in the analogous five-membered cyclometalated complex [Pt(bipy-H)(Me)(PPh_3)] (**11**),[26] in which bipy-H is a cyclometalated "rollover" bipyridine, is 79.61(9)°. Correspondingly, the angles involving phosphorus are larger than 90°, which seems reasonable considering the hindrance exerted by the PPh_3 group (N101–Pt1–C1 193.64°). The structure has a very slight pyramidal distortion, which is highlighted by the angle between the best planes calculated through N1–Pt–C108 and P1–Pt–C1 (1.2°). Moreover, the best plane drawn through the cyclometalated ligand has an angle of 3.8° with the fragment comprising the metal centre and the two other ligands. There are no unusual interactions or short contacts revealed in the packing of **5**. Overall, the distances and angles around the metal are typical of similar species, such as **11**.

The solid-state structure of complex **9** consists of discrete molecules separated by van der Waals distances, in the orthorhombic space group *Pbca*. The complex is planar, with the largest deviation from the best plane comprising the metal and its bounded atoms again found for C108, which is 0.061 Å away from the plane.

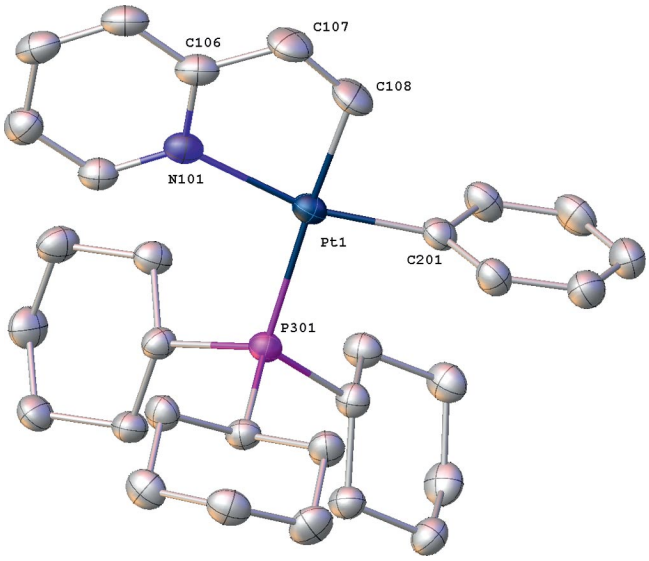

Figure 4. X-ray crystal structure of **9**. Thermal ellipsoids are drawn at 50% probability. Hydrogen atoms have been removed for clarity and only selected atoms are labelled. Selected bond lengths [Å] and angles [°]: Pt1–P301 2.3534(9); Pt1–N101 2.170(3); Pt1–C108 2.010(5); Pt1–C201 2.000(4); C107-C108 1.334(7); C106–C107 1.440(6); C106–N101 1.376(5); P301–Pt1–C201 91.9(1); C108–Pt1–C201 86.1(2); C108–Pt1–N101 78.2(2); N101–Pt1–P301 103.78(9); P301–Pt1–C108 175.1(1); N101–Pt1–C201 164.3(1).

Angles around the platinum are similar to those in [Pt(L–H)(CH_3)(PPh_3)]: the cyclometalated ligand has a bite angle of 78.21°, whereas the angles involving the PCy_3 are wider [N(101)–Pt(1)–C(108) = 195.69°], compared with **5**, due to the increased cone angle of the phosphane. Steric strain is somewhat relieved by the presence of the phenyl group, which bends away from the phosphane taking advantage of its almost perpendicular coordination with respect to the cyclometalated plane.

The structure of **9** has a slight pyramidal distortion, highlighted by the angle between the planes passing through N(101)–Pt(1)–C(108) and P(301)–Pt(1)–C(201) of only 4.5°. Moreover, the best plane drawn through the cyclometalated ligand (all eight non-hydrogen atoms) has an angle of 6.3° with the fragment comprising the metal centre and the two other donors (N101 and C201). No unusual interactions due to packing or particular contacts were noted.

Electronic Spectroscopy and Electrochemical Behaviour

[Pt(L–H)(Me)(PPh_3)] (**5**) and [Pt(L–H)(Cl)(PPh_3)] (**10**) were characterised by UV/Vis spectroscopy in CH_2Cl_2 solution. Both derivatives showed spin-allowed π–π* ligand-centred transitions at 237 ($\varepsilon \approx 18000\ mol^{-1}\ L\,cm^{-1}$) and 279 nm (shoulder) for **5** and 265 ($\varepsilon \approx 10000\ mol^{-1}\ L\,cm^{-1}$) and 292 nm (shoulder) for **10**. Furthermore, in the lower energy region of the spectra, weaker transitions were evident that were ascribed to d_{Pt}–π* metal-to-ligand charge-transfers; these bands occurred at 336 ($\varepsilon \approx 3000\ mol^{-1}\ L\,cm^{-1}$) and 386 nm ($\varepsilon \approx 2500\ mol^{-1}\ L\,cm^{-1}$) for **5**, and 400 ($\varepsilon \approx$

2000 mol^{-1} L cm^{-1}) and 420 nm (shoulder) for **10**. Analysis of UV/Vis spectra allowed evaluation of the *E*g values for **5** and **10** as 2.88 and 2.81 eV, respectively.

The electrochemical behaviour of **5** and **10** was investigated by cyclic voltammetry in CH_2Cl_2/$TEAPF_6$ (0.1 M) solvent system, with a Pt (Figure 5) and a GC working electrode. No reductive processes were evident in the available potential range. Both derivatives show an anodic process, located at 1.14 V on Pt (1.03 V on GC) and 1.45 V on Pt (1.43 V on GC), respectively, that were irreversible on the experimental time-scale (20÷500 mV s^{-1}). The process can reasonably be assumed to stem from mono-electronic charge transfer located mainly on the metal centre, with a chemical reaction following the charge transfer.[27] Because Pt^{III} complexes are unstable species, oxidation processes that are mainly located on the metal centre are expected to be irreversible. Furthermore, oxidation processes in N^C complexes may also involve the heteroatom and are irreversible.[28] A comparison of the responses confirms that in the Me derivative the metal centre is more electron-rich than in the Cl derivative, as suggested from the different electron-withdrawing/donating ability of the Me and Cl substituents. As confirmation, the HOMO energy values obtained from the cyclic voltammetric responses on the Pt working electrode are –5.22 eV for **5** and –5.44 eV for **10**. Evaluation of the LUMO energy from ($Eg + E_{HOMO}$) confirms that the cyclometalated ligand in **5** has a higher electron density than in **10**.

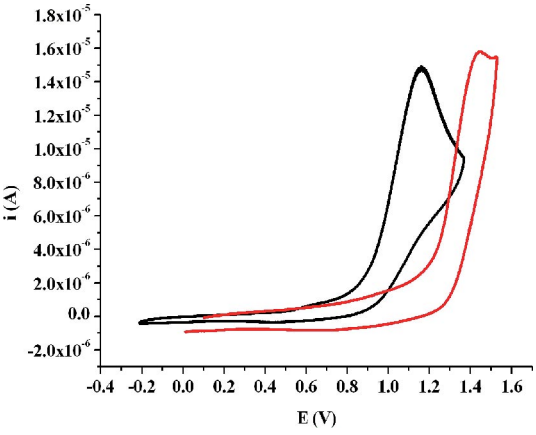

Figure 5. Cyclic voltammetric responses of [Pt(L–H)(Me)(PPh_3)] (**5**; black line) and [Pt(L–H)(Cl)(PPh_3)] (**10**; red line) in CH_2Cl_2/$TEAPF_6$ (0.1 M) solvent system on a Pt working electrode. Potential scan rate 100 mV s^{-1}. Potential values referred to SCE.

Cyclometalation, Delocalisation and Aromaticity

Five-membered cyclometalated rings are often reported to have a certain degree of aromaticity. Such metallacycles, which include metallapyrroles,[29] metallafurans[30] and metallathiophenes,[31] have received much attention in recent years. Among the vast number of systems, cyclometalated 2-vinylpyridine may be described as a metallaindolizine, and a 3-ruthenaindolizine complex has been recently reported by Esteruelas and co-workers.[32] Analysis of the five-membered metallacycle in metallapyrroles and metallaindolizines (**A** and **B**, see below) show elongated C1–C2 bonds associated with short C2–C3 bond lengths, in particular when compared to non-cyclic analogous species (species **C**, see below). Short M–N and M–C1 bond lengths have also been reported for these delocalised metallacycles.

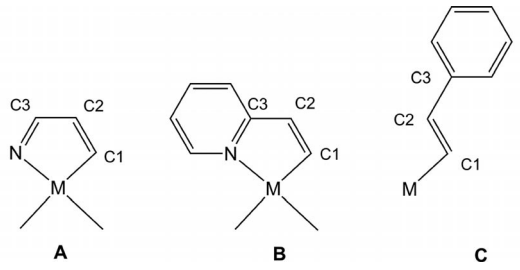

The analysis of bond lengths in compounds **5** and **9** shows a short C1–C2 bond in **5** [1.313(5) Å] and a longer bond [1.334(7) Å] in **9**. The C2–C3 bond length is shorter than expected for a single C–C sp^2 bond [1.442(5) and 1.440(6) Å, respectively], and is close to an aromatic C–C bond length. For comparison, in the aromatic ruthenaindolizine complex [Ru(L–H)(PR_3)(Tp)] [R = isopropyl, Tp = hydridotris(pyrazolyl)borate],[32] C1–C2 1.35(2) and C2–C3 1.428(3) Å, and in the non-cyclic complex [Ru(CH_3){(*E*)-CH=CHPh}$(CO)_2$($PiPr_3$)$_2$] (species C, above), C1–C2 1.311(6) Å and C2–C3 1.497(5) Å.[33] Analysis of the Pt–C1 bond in **5** and **9** (2.013 and 2.010 Å, respectively) reveal normal values for Pt–C bonds in a five-membered cycle; however, partial delocalisation should always be taken into account.

In contrast, in non-cyclic complexes or in non-planar cyclometalates (e.g., six- or seven-membered cycles), Pt–C(sp^2) bonds are usually longer. As an example of Pt–C(sp^2) bonds *trans* to PPh_3 we may cite the non-cyclic *trans*-Pt(H)(SAr)$(PPh_3)_2$ (Ar = C_6H_4Cl-*p*),[34] which has a Pt–C bond length of 2.066 Å, and the non-planar six-membered metallacycle [{η^6–2-MeBTPt(PPh_3)$_2$}Mn$(CO)_3$]-BF_4 (BT = benzothiophene),[35] in which the Pt–C bond length is 2.056 Å. Interestingly, the Pt–C1 bond lengths in **5** and **9** are short even when compared with the analogous cyclometalated complex [Pt(NC)(Me)(PPh_3)] (NC = cyclometalated "rollover" 2,2′-bipyridine), in which the same bond is 2.043(3) Å.[26]

On the whole, the metallacycle in complexes **5** and **9** seems to have a certain degree of delocalisation, with short C2–C3 and Pt–C1 bonds; in contrast, in complex **9** the C1–C2 bond seems to be slightly elongated.

Interestingly, ^1H NMR spectra show large ^{195}Pt–^1H coupling constants for the olefinic protons in the electron-rich complexes (e.g., **2** and **5**) and weaker couplings in the electron-poorer compounds (e.g., **4** and **10**), which may be correlated with partial π-delocalisation favoured by electron density on the metal. In agreement with such partial π-delocalisation, ^1H NMR signals of Hα and Hβ in most of the complexes reported here are strongly deshielded, resonating in the aromatic region of the spectra.

Comparison with 2-Ethylpyridine

In an attempt to extend the study, we also tried to cyclometalate 2-ethylpyridine (L′), to compare C(sp^2)–H and C(sp^3)–H bond activation in the formation of five-membered cyclometalated rings. However, we were not able to cyclometalate L′ starting from *cis*-[Pt(CH_3)$_2$(DMSO)$_2$], and only obtained the adduct [Pt(L′)(Me)$_2$(DMSO)] (**12**), a species analogous to complex **1**.

Complex **12** was characterised based mainly on its ^{1}H NMR spectrum. The H-6 proton (δ = 8.70 ppm) showed satellites that were indicative of coordination of the nitrogen ($^3J_{Pt,H}$ = 20 Hz) *trans* to a carbon atom. Two coordinated methyl groups were present: on the basis of ^{195}Pt–^{1}H coupling constants and a comparison with complex **1**, the signals may be assigned to a methyl *trans* to N (δ = 0.40 ppm; $^3J_{Pt,H}$ = 84.9 Hz) and to a methyl *trans* to DMSO (δ = 0.43 ppm; $^3J_{Pt,H}$ = 77.9 Hz). In contrast to complex **1**, the DMSO ligand generated two singlets with satellites (δ = 2.87 ppm, $J_{Pt,H}$ = 15.3 Hz; δ = 2.83 ppm, $J_{Pt,H}$ = 15.3 Hz), indicating that the methyl groups are diastereotopic. This implies that the pyridine does not rotate around the Pt–N bond on the NMR time-scale, in contrast to the motion proposed for complex **1**. Hence, on the NMR time-scale, complex **12** is a chiral species (an example of planar chirality). Accordingly, the CH_2 protons are also diastereotopic, and appear as two multiplets at δ = 3.51 and 3.45 ppm, each integrating one proton; both signals are strongly shifted with respect to the free ligand (δ = 2.76 ppm).

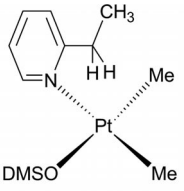

12

Attempts to obtain cyclometalated complexes analogous to **2** failed, even at high temperatures and after prolonged reaction times, indicating that C–H bond activation in the ethyl substituent is not easy. It is worth noting that the corresponding 2,2′-bipyridine ligand, 6-ethyl-2,2′-bipyridine, reacts easily with Pt^{II} complexes to give the terdentate cyclometalated complex [Pt(N,N,C)Cl].[18b]

Conclusions

We have shown that 2-vinylpyridine easily gives five-membered cycloplatinated complexes. At variance with the well-known cyclometalating pro-ligand 2-phenylpyridine, however, cyclometalation of 2-vinylpyridine requires harsher conditions. The species obtained are extremely stable and show interesting features, such as remarkable ^{195}Pt–^{1}H coupling constants inside the metallacycle. Such coupling constants are particularly large for the electron-rich complexes of the series (e.g., **2** and **5**) and this may due to partial π-delocalisation inside the cycle.

Experimental Section

General: All the solvents were purified and dried according to standard procedures.[36] *cis*-[Pt(Me)$_2$(DMSO)$_2$], *trans*-[Pt(Me)(Cl)-(DMSO)$_2$] and [Pt(Ph)$_2$(DMSO)$_2$] were synthesised according to reported procedures.[37] Elemental analyses were performed with a Perkin–Elmer elemental analyzer 240B.

^{1}H, ^{13}C{^{1}H} and ^{31}P{^{1}H} NMR spectra were recorded with Varian VXR 300 or Bruker Avance III 400 spectrometers. Chemical shifts are given in ppm relative to internal TMS for ^{1}H and ^{13}C{^{1}H} and external 85% H_3PO_4 for ^{31}P{^{1}H}; *J* values are given in Hz. ^{1}H-^{1}H COSY, ^{1}H-^{1}H NOESY and ^{1}H 1D-NOE experiments were performed by using standard pulse sequences.

UV/Vis spectra were recorded with a Fulltech T80+ spectrophotometer. Cyclic voltammetric tests were performed with a computerised electrochemical system CHI-650 (CH Instruments, Austin, TX, USA) using its specific software, employing a single-compartment, three-electrode cell, at room temperature, under an Ar atmosphere, at a potential scan rate of 100 mV s^{-1}. A 2 mm diameter Pt or a 3 mm diameter glassy carbon (GC) disk electrode was used as working electrode, an aqueous SCE with suitable salt bridge was used as the reference electrode, and a graphite rod was used as the auxiliary electrode. All the experiments were carried out in CH_2Cl_2 (Sigma–Aldrich, anhydrous, ≥ 99.8%) using 0.1 M tetraethylammonium hexafluorophosphate ($TEAPF_6$, Sigma–Aldrich, for electrochemical analysis, ≥ 99.0%) as supporting electrolyte, with sample concentration of ca. 2×10^{-3} M. Energy-gap values (*Eg*) were evaluated from the λ_{onset} in the UV/Vis spectra. HOMO energy values were evaluated from the equation E_{HOMO} [eV] = $-e(E_{onset} + 4.4)$.[38]

DFT calculations were carried out with the Firefly QC package,[39] which is partially based on the GAMESS (US)[40] source code. Full details are given in the Supporting Information.

Preparations

[Pt(CH_3)$_2$(L)(DMSO)] (1): To a solution of *cis*-[Pt(CH_3)$_2$-(DMSO)$_2$] in [D$_6$]acetone in an NMR tube was added an excess of 2-vinylpyridine. The reaction was followed in solution by means of ^{1}H NMR spectroscopy, at 25 and 40 °C. ^{1}H NMR (400 MHz, [D$_6$]-acetone, room temp.): δ = 8.83 (ddd sat, $J_{H,H}$ = 5.5, 1.6, 1.0 Hz, $J_{Pt,H}$ = 20 Hz, 1 H, H-6), 8.21 (dd sat, $J_{H,H}$ = 17.8, 11.3 Hz, $J_{Pt,H}$ = 10 Hz, 1 H, Hα), 7.91 (m, 2 H, H-3 + H-5), 7.37 (td, 1 H, H-4), 6.12 (d, $J_{H,H}$ = 17.8 Hz, 1 H, Hβ_{trans}), 5.70 (d, $J_{H,H}$ = 11.3 Hz, 1 H, Hβ_{cis}), 2.79 (s sat, $J_{Pt,H}$ = 14.4 Hz, 6 H, DMSO), 0.48 (s sat, $^2J_{Pt,H}$ = 88.8 Hz, 3 H, CH_3), 0.33 (s sat, $^2J_{Pt,H}$ = 79.2 Hz, 3 H, CH_3) ppm. ^{1}H NMR (400 MHz, [D$_6$]acetone, 40 °C): δ (selected signals) = 0.17 (CH_4), 9.40 (dd sat, $J_{H,H}$ = 5.5, $J_{Pt,H}$ = 11 Hz, 1 H, H-6), 6.93 (d, $J_{H,H}$ = 8.8 Hz, 1 H, Hβ), 0.68 (s sat, $^2J_{Pt,H}$ = 82 Hz, 3 H, CH_3) ppm.

[Pt(L–H)(CH_3)(DMSO)] (2): To a solution of *cis*-[Pt(CH_3)$_2$-(DMSO)$_2$] (0.264 mmol, 1 equiv.) in toluene (15 mL) was added 2-vinylpyridine (34 μL, 0.316 mmol, 1.2 equiv.). The solution was stirred under a nitrogen atmosphere for 2 h at 80 °C, then evaporated to dryness and vacuum pumped to give an analytical sample as a yellow solid, yield 88.1 mg (85%). ^{1}H NMR (300 MHz, $CDCl_3$): δ = 9.24 (d sat, $J_{H,H}$ = 5.5 Hz, $^3J_{Pt,H}$ = 12 Hz, 1 H, H-6), 7.63 (td, $^3J_{H,H}$ = 7.5 Hz, $^4J_{H,H}$ = 1.6 Hz, 1 H, H-4), 7.42 (d sat, $^3J_{H,H}$ = 8.7 Hz, $^2J_{Pt,H}$ = 171 Hz, 1 H, Hβ), 7.08 (d, $^3J_{H,H}$ = 7.5 Hz, 1 H, H-3), 7.00 (m, 1 H, H-5), 6.94 (d sat, $^3J_{H,H}$ = 8.7 Hz, $^3J_{Pt,H}$ = 108 Hz, 1 H, Hα), 3.07 (s sat, $^3J_{Pt,H}$ = 16.8 Hz, 6 H, CH_3 of DMSO), 0.69 (s sat, $^2J_{Pt,H}$ = 82.5 Hz, 3 H, Pt-CH_3) ppm. ^{13}C NMR (75.4 MHz, $CDCl_3$): δ = 166.9 (s sat, $J_{Pt,C}$ = 115 Hz, C2), 163.2 (s sat, $J_{Pt,C}$ = 1035 Hz, Cβ), 150.5 (s sat, $^2J_{Pt,C}$ = 15.6 Hz, C6), 139.3,

138.4 (s sat, $J_{Pt,C}$ = 4.0 Hz, C4), 121.2 (s sat, $J_{Pt,C}$ = 5.2 Hz, C3 or C5), 119.5 (s sat, $J_{Pt,C}$ = 18.6 Hz, C3 or C5), 43.5 (s sat, $^2J_{Pt,C}$ = 40 Hz, CH_3 of DMSO), –19.9 (s sat, $^1J_{Pt,C}$ = 756 Hz, Pt-CH_3) ppm. $C_{10}H_{15}NOPtS$ (392.38): calcd. C 30.61, H 3.85, N 3.57; found C 30.84, H 3.63, N 3.68.

[Pt(L–H)(Ph)(DMSO)] (3): Complex **3** was synthesised as described for complex **2**, using *cis*-[$Pt(Ph)_2(DMSO)_2$] in place of *cis*-[$Pt(CH_3)_2(DMSO)_2$], at 80 °C for 3 h, yield 70%; m.p. 133 °C. ^{1}H NMR (300 MHz, $CDCl_3$): δ = 9.29 (d sat, $^3J_{H,H}$ = 5.4 Hz, $^3J_{Pt,H}$ = 12.6 Hz, 1 H, H-6), 7.72 (td, $^3J_{H,H}$ = 8.7 Hz, 1 H, H-4), 7.39 (m sat, $^3J_{Pt,H}$ = 71 Hz, 2 H, partially overlapping, H_o), 7.38 (d with sat, $^3J_{H,H}$ = 7.9 Hz, $^2J_{Pt,H}$ = 180 Hz, 1 H, partially overlapping, Hβ), 7.20 (d, $^3J_{H,H}$ = 7.9 Hz, 1 H, H-3), 7.17 (td, 1 H, H-5), 7.06 (m, 2 H, H_m), 6.95 (td, 1 H, H_p), 6.90 (d sat, $^3J_{H,H}$ = 8.7 Hz, $^4J_{Pt,H}$ = 118 Hz, 1 H, Hβ), 2.89 [s sat, $^2J_{Pt,H}$ = 16.8 Hz, 6 H, CH_3 of DMSO] ppm. $C_{15}H_{17}NOPtS$ (454.35): C, 39.64; H, 3.77; N, 3.08; found C, 39.42; H, 3.62, N, 3.29.

[Pt(L–H)(Cl)(DMSO)] (4); Method A: To a solution of *trans*-[$Pt(CH_3)(Cl)(DMSO)_2$] (165 mg, 0.410 mmol, 1 equiv.) in acetone (10 mL) was added under vigorous stirring 2-vinylpyridine (48 mg, 0.456 mmol, 1.10 equiv.). The solution was stirred at 55 °C for 6 h, then concentrated to small volume and treated with *n*-hexane. The precipitate formed was filtered off, washed with *n*-hexane and vacuum pumped to give an analytical sample as a yellow solid, yield 152.3 mg (90%).

Method B: To a solution of **2** in acetone was added aqueous 0.1 M HCl (1:1 Pt/acid molar ratio). The mixture was stirred at room temperature for 1 h then evaporated to dryness. Complex **4** was obtained by crystallisation of the resulting crude material from CH_2Cl_2/*n*-hexane, yield 90%, m.p. 124 °C. ^{1}H NMR (300 MHz, $CDCl_3$): δ = 9.10 (ddd sat, $J_{H,H}$ = 5.8, 1.6, 0.8 Hz, $^3J_{Pt,H}$ = 33 Hz, 1 H, H-6), 7.75 (td, $^3J_{H,H}$ = 7.7 Hz, 1 H, H-4), 7.26 (d sat, $^3J_{H,H}$ = 7.5 Hz, $^3J_{Pt,H}$ = 84 Hz, 1 H, Hα), 7.18 (d, $^3J_{H,H}$ = 7.7 Hz, 1 H, H-3), 7.14 (m, 1 H, H-5), 6.65 (d sat, $^3J_{H,H}$ = 7.5 Hz, $^2J_{Pt,H}$ = 97 Hz, 1 H, Hβ), 3.54 [s sat, $^3J_{Pt,H}$ = 25.6 Hz, 6 H, CH_3 of DMSO] ppm. $C_9H_{12}ClNOPtS$ (412.80): calcd. C 26.19, H 2.93, N 3.39; found C 26.32, H 2.68, N 3.29.

General Method for the Synthesis of Complexes [Pt(L–H)(R)(L)] (R = Me, Ph, L = Phosphane or CO) 5–9; Method A (one pot): To a solution of [$Pt(R)_2(DMSO)_2$] (R = Me or Ph, 0.25 mmol, 1 equiv.) in toluene (10 mL), was added under a nitrogen atmosphere, 2-vinylpyridine (34 μL, 0.316 mmol, 1.26 equiv.). The solution was stirred at 80 °C for 2 h, then heating was turned off and the phosphane (0.30 mmol, 1.2 equiv.) was added. The solution was stirred for 1 h, then concentrated to a small volume and treated with *n*-hexane. The precipitate formed was filtered off, washed with *n*-hexane and vacuum pumped to give the analytical sample.

[Pt(L–H)(Me)(PPh_3)] (5): Obtained by Method A (R = Me), yield 92%; m.p. 162 °C. ^{1}H NMR (300 MHz, $CDCl_3$): δ = 7.90 (dd sat, $^3J_{H,H}$ = 9.2 Hz, $^3J_{P,H}$ = 7.8 Hz, $^2J_{Pt,H}$ = 163 Hz, 1 H, Hβ), 7.65–7.42 (m, 18 H, Ar-H), 7.33 (dd sat, $^3J_{H,H}$ = 9.2 Hz, $^4J_{P,H}$ = 15.2 Hz, $^3J_{Pt,H}$ = 94 Hz, 1 H, Hα), 7.14 (d, $J_{H,H}$ = 7.8 Hz, 1 H, H-3), 6.45 (t, $J_{H,H}$ = 6.3 Hz, 1 H), 0.80 (d sat, $^3J_{P,H}$ = 8.1, $^2J_{Pt-H}$ = 84 Hz, 3 H, Pt-CH_3) ppm. ^{31}P NMR (121.4 MHz, $CDCl_3$): δ = 28.5 (s sat, $^1J_{Pt,P}$ = 2020 Hz) ppm.

[Pt(L–H)(Me)(PCy_3)] (6): Obtained by Method A (R = Me), yield 95%. ^{1}H NMR ($CDCl_3$): δ = 8.46 (d sat, $^3J_{H,H}$ = 5.2 Hz, $^3J_{Pt,H}$ = 17.1 Hz, 1 H, H-6), 7.73 (dd, $J_{H,H}$ = 9.1 Hz, $J_{P,H}$ = 7.8 Hz, 1 H, $J_{Pt,H}$ = 155 Hz, Hβ), 7.62 (td, 1 H, H-4), 7.39 (dd, $J_{H,H}$ = 9.1 Hz, $J_{P,H}$ = 14.1 Hz, $J_{Pt,H}$ = 86 Hz, 1 H, Hα), 7.11 (t sat, $^3J_{H,H}$ = 8.2 Hz, 1 H), 6.90 (td, 1 H, H-5), 2.00–1.05 (m, 33 H, CH and CH_2 of PCy_3), 1.04 (d sat, $^3J_{P,H}$ = 6.0 Hz, $^2J_{Pt,H}$ = 84.9 Hz, 3 H, Pt-CH_3) ppm. ^{31}P NMR (121.4 MHz, $CDCl_3$): δ = 26.2 (s sat, $J_{Pt,P}$ = 1875 Hz) ppm.

[Pt(L–H)(Me)(CO)] (7): Obtained by Method B (R = Me). In this case, CO was bubbled into the solution for 1 h. ^{1}H NMR (300 MHz, $CDCl_3$): δ = 8.49 (d br. sat, $J_{H,H}$ = 5.4 Hz, $^3J_{Pt,H}$ = 16.2 Hz, 1 H, H-6), 7.12 (m, $J_{H,H}$ = 5.4 Hz, $J_{H,H}$ = 7.0 Hz, 1 H, H-5), 7.78 (td, $J_{H,H}$ = 2.0 Hz, $J_{H,H}$ = 7.0 Hz, 1 H, H-4), 7.17 (d, $J_{H,H}$ = 8.0 Hz, 1 H, H-3), 7.35 (d sat, $J_{H,H}$ = 9.7 Hz, $^2J_{Pt,H}$ = 156 Hz, 1 H, Hβ), 7.26 (d sat, $J_{H,H}$ = 9.7 Hz, $^3J_{Pt,H}$ = 106 Hz, 1 H, Hα), 1.21 (s sat, $^2J_{Pt,H}$ = 87.0 Hz, 3 H, Pt-CH_3) ppm. IR (Nujol): $\tilde{\nu}$ = 2046 (vs, ν CO) cm^{-1}.

[Pt(L–H)(Ph)(PPh_3)] (8): Obtained by Method A, yield 70%; m.p. 154 °C. ^{1}H NMR (300 MHz, $CDCl_3$): δ = 7.79 (td, $^3J_{H,H}$ = 7.7 Hz, $^3J_{H,H}$ = 1.5 Hz, 1 H, H-4), 7.70–7.20 (m, 21 H, Ar-H, Hβ), 7.01 [d sat, $^3J_{H,H}$ = 6.3 Hz, $^3J_{Pt,H}$ = 70.1 Hz, 2 H, H_o(Ph)], 6.60 (m, 3 H), 6.43 (td, $^3J_{H,H}$ = 5.7 Hz, $^3J_{H,H}$ = 1.5 Hz, 1 H, H-5) ppm. ^{31}P NMR (121.4 MHz, $CDCl_3$): δ = 31.46 (s sat, $^1J_{Pt,P}$ = 1990 Hz) ppm.

[Pt(L–H)(Ph)(PCy_3)] (9): Obtained by Method A, yield 75%; m.p. 147 °C. ^{1}H NMR (300 MHz, $CDCl_3$): 8.43 (d sat, $^3J_{H,H}$ = 5.4 Hz, $^3J_{Pt,H}$ = 17.0 Hz, 1 H, H-6), 7.59 (td, $^3J_{H,H}$ = 7.6 Hz, $^3J_{H,H}$ = 1.3 Hz, 1 H, H-4), 7.33 (d, 1 H, Hα), 7.01 (d, $^3J_{H,H}$ = 7.6 Hz, 1 H, H-3), 6.90 (m, 1 H, H-5), 6.71 (d sat, 1 H, Hβ), 2.00–0.90 (m, 11 H, PCy_3) ppm. ^{31}P NMR (121.4 MHz, $CDCl_3$): δ = 24.1 (s sat, $^1J_{Pt,P}$ = 1843 Hz) ppm.

[Pt(L–H)(Cl)(PPh_3)] (10): Obtained by Method B, yield 90%; m.p. 164 °C. ^{1}H NMR (300 MHz, $CDCl_3$): δ = 9.45 (s br. sat, $^3J_{Pt,H}$ = 26.3 Hz, 1 H, H-6), 7.77–7.67 (m, 7 H, H-4, H_o(PPh_3)), 7.49–7.40 [m, 9 H, H_m, H_p (PPh_3)], 7.20 (m, $^2J_{H,H}$ = 6.8 Hz, 1 H, H-5), 7.12 (d, $^2J_{H,H}$ = 7.3 Hz, 1 H, H-3), 6.63 (dd sat, $^3J_{H,H}$ = 8.3 Hz, $^3J_{Pt,H}$ = 95 Hz, $^4J_{P,H}$ = 0.5 Hz, 1 H, Hα), 6.39 (t sat, $^3J_{H,H}$ = $^3J_{P,H}$ = 8.3 Hz, $^2J_{Pt,H}$ = 139 Hz, 1 H, Hβ) ppm. ^{31}P NMR (121.4 MHz, $CDCl_3$): δ = 17.9 (s sat, $J_{Pt,P}$ = 4194 Hz) ppm. $C_{25}H_{21}ClNPPt$ (596.95): calcd. C 51.42; H 3.62; N 2.39; found C 50.20; H 3.29; N 2.51.

[Pt(L′)($Me)_2$(DMSO)] (12): Complex **12** may be obtained as complexes **1** or **2**, using 2-ethylpyridine (L′) in place of 2-vinylpyridine (L). ^{1}H NMR (300 MHz, [D_6]acetone): δ = 8.70 (dd sat, 1 H, $^3J_{H,H}$ = 5.6 Hz, $J_{Pt,H}$ = 20 Hz, H-6), 7.56 (td, $^3J_{H,H}$ = 7.8 Hz, 1 H, H-4), 7.34 (d, $^3J_{H,H}$ = 7.8 Hz, 1 H, H-3), 7.09 (m, 1 H, H-5), 3.51 (m, $^2J_{H,H}$ = 15.0 Hz, $^3J_{H,H}$ = 7.5 Hz, 1 H, CH_2), 3.45 (m, $^2J_{H,H}$ = 15.0 Hz, $^3J_{H,H}$ = 7.5 Hz, 1 H, CH_2), 2.87 (s sat, $^3J_{Pt,H}$ = 15.3 Hz, 3 H, DMSO), 2.83 (s sat, $^3J_{Pt,H}$ = 15.3 Hz, 3 H, DMSO), 1.36 (t, $^3J_{H,H}$ = 7.5 Hz, 3 H, CH_3CH_2), 0.40 ppm (s sat, $^3J_{Pt,H}$ = 84.9 Hz, 3 H, Pt-CH_3), 0.43 ppm (s sat, $^3J_{Pt,H}$ = 77.9 Hz, 3 H, Pt-CH_3) ppm.

X-ray Experimental Data

Complex 5: Single crystals of $C_{26}H_{24}NPPt$ (**5**) were grown from acetone. A suitable crystal was selected and mounted on a glass fibre with Fromblin oil and placed on an Oxford Diffraction Xcalibur Gemini diffractometer with a Ruby CCD area detector. The crystal was kept at 150(2) K during data collection. The structure was solved by using Olex2,[41] with the XS[42] structure solution program using direct methods and refined with the ShelXL[42] refinement package using least squares minimisation (Table 1).

Complex 9: Single crystals of $C_{31}H_{44}NPPt$ (**9**) were grown from acetone. A suitable crystal was selected and mounted on a glass fibre with Fromblin oil and placed on an Oxford Diffraction Xcalibur Gemini diffractometer with a Ruby CCD area detector. The structure was solved by using Olex2,[41] with the XS[42] structure solution program using direct methods and refined with the

Table 1. X-ray data for complexes **5** and **9**.

	5	**9**
Crystal shape	brown block	brown block
Dimensions [mm]	$0.30 \times 0.30 \times 0.22$	$0.20 \times 0.04 \times 0.02$
Empirical formula	$C_{26}H_{24}NPPt$	$C_{31}H_{44}NPPt$
M	576.52	656.73
Crystal system	monoclinic	orthorhombic
Space group	$P2_1/n$	$Pbca$
a [Å]	9.33289(13)	8.64617(12)
b [Å]	19.1459(2)	18.0240(2)
c [Å]	12.87984(19)	35.5920(5)
α [°]	90	90
β [°]	101.3736(14)	90
γ [°]	90	90
U [Å^3]	2256.26(5)	5546.62(13)
T [K]	150(2)	150(2)
Z	4	8
λ [Å]	0.71073	1.54184
D(calcd.) [Mg/m^3]	1.697	1.573
F(000)	1120	2640
μ [mm^{-1}]	6.301 (Mo-K_α)	10.135 (Cu-K_α)
θmax. [°]	31.45	77.56
Reflections measured	26371	20284
Unique data	6885	5794
R(int)	0.0259	0.0276
Min./max. transmission factors	0.50/1.00	0.57/1.00

ShelXL[42] refinement package using least squares minimisation (Table 1).

CCDC-980421 (for **5**) and -980422 (for **9**) contain the supplementary crystallographic data for this paper. These data can be obtained free of charge from The Cambridge Crystallographic Data Centre via www.ccdc.cam.ac.uk/data_request/cif.

Supporting Information (see footnote on the first page of this article): Coordinates of the DFT-optimized structures.

Acknowledgments

Financial support from Università di Sassari (FAR) is gratefully acknowledged. L. M. gratefully acknowledges a PhD fund, financed on POR/FSE 2007-2013, from Regione Autonoma della Sardegna. The authors acknowledge support from the Advantage West Midlands (AWM) (partially funded by the European Regional Development Fund) for the purchase of the XRD system that was used to solve the crystal structure of **5** and **9**.

[1] a) M. Albrecht, *Chem. Rev.* **2010**, *110*, 576–623; b) A. D. Ryabov, *Chem. Rev.* **1990**, *90*, 403–424.

[2] a) V. K.-M. Au, W. H. Lam, W.-T. Wong, V. W.-W. Yam, *Inorg. Chem.* **2012**, *51*, 7537–7545; b) S. Moromizato, Y. Hisamatsu, T. Suzuki, Y. Matsuo, R. Abe, S. Aoki, *Inorg. Chem.* **2012**, *51*, 12697–12706; c) P. G. Bomben, T. J. Gordon, E. Schott, C. P. Berlinguette, *Angew. Chem. Int. Ed.* **2011**, *50*, 10682–10685; *Angew. Chem.* **2011**, *123*, 10870; d) S. T. Madrahimov, J. F. Hartwig, *J. Am. Chem. Soc.* **2012**, *134*, 8136–8147; e) P. S. Hanley, J. F. Hartwig, *J. Am. Chem. Soc.* **2011**, *133*, 15661–15673; f) M. Zhou, D. Balcells, A. R. Parent, R. H. Crabtree, O. Eisenstein, *ACS Catal.* **2012**, *2*, 208–218.

[3] For examples, see: a) Á. Díez, E. Lalinde, M. T. Moreno, *Coord. Chem. Rev.* **2011**, *255*, 2426–2447; b) Y. Chen, K. Li, W. Lu, S. S.-Y. Chui, C.-W. Ma, C.-M. Che, *Angew. Chem. Int. Ed.* **2009**, *48*, 9909–9913; *Angew. Chem.* **2009**, *121*, 10093; c) J. R. Berenguer, E. Lalinde, M. T. Moreno, S. Sánchez, J. Torroba, *Inorg. Chem.* **2012**, *51*, 11665–11679; d) T. Okada, I. M. El-Mehasseb, M. Kodaka, T. Tomohiro, K.-I. Okamoto, H. Okuno, *J. Med. Chem.* **2001**, *44*, 4661–4667.

[4] For example, see: M. Albrecht, G. van Koten, *Angew. Chem. Int. Ed.* **2001**, *40*, 3750–3781; *Angew. Chem.* **2001**, *113*, 3866.

[5] a) C. P. Newman, K. Casey-Green, G. J. Clarkson, G. W. V. Cave, W. Errington, J. P. Rourke, *Dalton Trans.* **2007**, 3170–3182.

[6] For examples, see: a) P. Jolliet, M. Gianini, A. von Zelewsky, G. Bernardinelli, H. Stoeckli-Evans, *Inorg. Chem.* **1996**, *35*, 4883–4888; b) F. Niedermair, K. Waich, S. Kappaun, T. Mayr, G. Trimmel, K. Mereiter, C. Slugovc, *Inorg. Chim. Acta* **2007**, *360*, 2767–2777; c) T. Yagyu, J.-I. Ohashi, M. Maeda, *Organometallics* **2007**, *26*, 2383–2391.

[7] a) A. Kasahara, K. Tanaka, T. Izumi, *Bull. Chem. Soc. Jpn.* **1969**, *42*, 1702–1704; b) G. R. Newkome, K. J. Theriot, B. K. Cheskin, D. W. Evans, G. R. Baker, *Organometallics* **1990**, *9*, 1375–1379.

[8] A. G. Wong-Foy, L. M. Henling, M. Day, J. A. Labinger, J. E. Bercaw, *J. Mol. Catal. A* **2002**, *189*, 3–16.

[9] H.-F. Klein, S. Camadanli, R. Beck, D. Leukel, U. Flörke, *Angew. Chem. Int. Ed.* **2005**, *44*, 975–977; *Angew. Chem.* **2005**, *117*, 997.

[10] a) R. J. Foot, B. T. Heaton, *J. Chem. Soc., Chem. Commun.* **1973**, 838–839; b) R. J. Foot, B. T. Heaton, *J. Chem. Soc., Dalton Trans.* **1979**, 295–298; c) J. Müller, C. Hirsch, K. Ha, *Z. Anorg. Allg. Chem.* **2003**, *629*, 2180–2185.

[11] J. Navarro, E. Sola, M. Martín, I. T. Dobrinovitch, F. J. Lahoz, L. A. Oro, *Organometallics* **2004**, *23*, 1908–1917.

[12] a) K. Hiraki, N. Ochi, Y. Sasada, H. Hayashida, Y. Fuchita, S. Yamanaka, *J. Chem. Soc., Dalton Trans.* **1985**, 873–877; b) G. Jia, D. W. Meek, J. C. Gallucci, *Organometallics* **1990**, *9*, 2549–2555; c) J. N. Coalter III, W. E. Streib, K. G. Caulton, *Inorg. Chem.* **2000**, *39*, 3749–3756; d) M. L. Buil, M. A. Esteruelas, E. Goni, M. Oliván, E. Oñate, *Organometallics* **2006**, *25*, 3076–3083; e) L. Zhang, L. Dang, T. Bin Wen, H. H.-Y. Sung, I. D. Williams, Z. Lin, G. Jia, *Organometallics* **2007**, *26*, 2849–2860; f) K. A. Azam, D. W. Bennett, M. R. Hassan, D. T. Haworth, G. Hogarth, S. E. Kabir, S. V. Lindeman, L. Salassa, S. R. Simi, T. A. Siddiquee, *Organometallics* **2008**, *27*, 5163–5166.

[13] a) K. Burgess, H. D. Holden, B. F. G. Johnson, J. Lewis, M. B. Hursthouse, N. P. C. Walker, A. J. Deeming, P. J. Manning, R. Peters, *J. Chem. Soc., Dalton Trans.* **1985**, 85–90; b) W.-Y. Wong, W.-T. Wong, *J. Organomet. Chem.* **1996**, *513*, 27–29; c) J. P.-K. Lau, W.-T. Wong, *Inorg. Chem. Commun.* **2003**, *6*, 174–177; d) P. Barrio, M. A. Esteruelas, E. Oñate, *Organometallics* **2004**, *23*, 3627–3639; e) B. Eguillor, M. A. Esteruelas, M. Oliván, E. Oñate, *Organometallics* **2005**, *24*, 1428–1438; f) M. A. Esteruelas, F. J. Fernández-Alvarez, M. Oliván, E. Oñate, *J. Am. Chem. Soc.* **2006**, *128*, 4596–4597.

[14] O. V. Ozerov, M. Pink, L. A. Watson, K. G. Caulton, *J. Am. Chem. Soc.* **2004**, *126*, 2105–2113.

[15] M. A. Cinellu, F. Cocco, G. Minghetti, S. Stoccoro, A. Zucca, M. Manassero, *J. Organomet. Chem.* **2009**, *694*, 2949–2955.

[16] For examples, see: a) H. Masui, *Coord. Chem. Rev.* **2001**, *219*, 957–992; b) M. Ghedini, I. Aiello, A. Crispini, A. Golemme, M. La Deda, D. Pucci, *Coord. Chem. Rev.* **2006**, *250*, 1373–1390.

[17] For example, see: a) G. Minghetti, A. Zucca, S. Stoccoro, M. A. Cinellu, M. Manassero, M. Sansoni, *J. Organomet. Chem.* **1994**, *481*, 195–204; b) G. Minghetti, A. Doppiu, S. Stoccoro, A. Zucca, M. A. Cinellu, M. Manassero, M. Sansoni, *Eur. J. Inorg. Chem.* **2002**, 431–438.

[18] For example, see: a) G. Minghetti, M. A. Cinellu, S. Stoccoro, A. Zucca, M. Manassero, *J. Chem. Soc., Dalton Trans.* **1995**, 777–781; b) A. Zucca, S. Stoccoro, M. A. Cinellu, G. Minghetti, M. Manassero, M. Sansoni, *Eur. J. Inorg. Chem.* **2002**, 3336–3346; c) A. Zucca, G. L. Petretto, M. L. Cabras, S. Stoccoro, M. A. Cinellu, M. Manassero, G. Minghetti, *J. Organomet. Chem.* **2009**, *694*, 3753–3761.

[19] G. Minghetti, S. Stoccoro, M. A. Cinellu, B. Soro, A. Zucca, *Organometallics* **2003**, *22*, 4770–4777.
[20] M. Brookhart, M. L. H. Green, G. Parkin, *Proc. Natl. Acad. Sci. USA* **2007**, *104*, 6908–6914.
[21] For example, see: A. Zucca, G. L. Petretto, S. Stoccoro, M. A. Cinellu, M. Manassero, C. Manassero, G. Minghetti, *Organometallics* **2009**, *28*, 2150–2159.
[22] A. Zucca, D. Cordeschi, L. Maidich, M. I. Pilo, E. Masolo, S. Stoccoro, M. A. Cinellu, S. Galli, *Inorg. Chem.* **2013**, *52*, 7717–7731.
[23] a) J. E. Huheey, E. A. Keiter, R. A. Keiter, O. K. Mehdi, *Inorganic Chemistry: Principles of Structure and Reactivity*, 4th ed., Pearson, **2006**; b) R. H. Crabtree, *The Organometallic Chemistry of the Transition Metals*, John Wiley & Sons, New York, **2005**.
[24] a) S. I. Gorelsky, *AOMix: Program for Molecular Orbital Analysis*, http://www.sg-chem.net/, v. 6.81, **2013**; b) S. I. Gorelsky, A. Lever, *J. Organomet. Chem.* **2001**, *635*, 187–196.
[25] J. S. Owen, J. A. Labinger, J. E. Bercaw, *J. Am. Chem. Soc.* **2004**, *126*, 8247–8255.
[26] A. Zucca, L. Maidich, L. Canu, G. L. Petretto, S. Stoccoro, M. A. Cinellu, G. J. Clarkson, J. P. Rourke, *Chem. Eur. J.* **2014**, DOI: 10.1002/chem.20130425.
[27] L. Chassot, E. Mueller, A. von Zelewsky, *Inorg. Chem.* **1984**, *23*, 4249–4253.
[28] P.-I. Kvam, M. V. Puzyk, V. S. Cotlyr, K. P. Balashev, J. Songstad, *Acta Chem. Scand.* **1995**, *49*, 645–652.
[29] For examples, see: a) Y. Alvarado, P. J. Daff, P. J. Pérez, M. L. Poveda, R. Sánchez-Delgado, E. Carmona, *Organometallics* **1996**, *15*, 2192–2194; b) P. Legzdins, S. A. Lumb, *Organometallics* **1997**, *16*, 1825–1827; c) T. Bolaño, R. Castarlenas, M. A. Esteruelas, E. Oñate, *J. Am. Chem. Soc.* **2006**, *128*, 3965–3973; d) J. R. Bleeke, P. Putprasert, T. Thananatthanachon, N. P. Rath, *Organometallics* **2008**, *27*, 5744–5747.
[30] For examples, see: a) B. Eguillor, M. A. Esteruelas, M. Oliván, E. Oñate, *Organometallics* **2004**, *23*, 6015–6024; b) X. Li, P. Chen, J. W. Faller, R. H. Crabtree, *Organometallics* **2005**, *24*, 4810–4815; c) Y. Lin, L. Gong, H. Xu, X. He, T. B. Wen, H. Xia, *Organometallics* **2009**, *28*, 1524–1533.
[31] a) J. R. Bleeke, M. F. Ortwerth, M. Y. Chiang, *Organometallics* **1993**, *12*, 985–987; b) G.-L. Lu, W. R. Roper, L. J. Wright, G. R. Clark, *J. Organomet. Chem.* **2005**, *690*, 972–981.
[32] M. A. Esteruelas, I. Fernández, S. Fuertes, A. M. López, E. Oñate, M. A. Sierra, *Organometallics* **2009**, *28*, 4876–4879.
[33] C. Bohanna, M. A. Esteruelas, F. J. Lahoz, E. Oñate, L. A. Oro, *Organometallics* **1995**, *14*, 4685–4696.
[34] A. Ohtaka, H. Kuniyasu, M. Kinomoto, H. Kurosawa, *J. Am. Chem. Soc.* **2002**, *124*, 14324–14325.
[35] C. A. Dullaghan, X. Zhang, D. L. Greene, G. B. Carpenter, D. A. Sweigart, C. Camiletti, E. Rajaseelan, *Organometallics* **1998**, *17*, 3316–3322.
[36] *Vogel's Textbook of Practical Organic Chemistry*, 5th edition, Longman Scientific and Technical Ed. Harlow, **1989**.
[37] a) C. Eaborn, K. Kundu, A. Pidcock, *J. Chem. Soc., Dalton Trans.* **1981**, 933–938; b) R. Romeo, L. Monsù Scolaro, V. Catalano, S. Achar, *Inorg. Synth.* **1998**, *32*, 153–158.
[38] Y. Li, Y. Cao, J. Gao, D. Wang, G. Yu, A. J. Heeger, *Synth. Met.* **1999**, *99*, 243–248.
[39] A. A. Granovsky, *Firefly*, v. 7.1.G; www http://classic.chem.msu.su/gran/firefly/index.html.
[40] M. W. Schmidt, K. K. Baldridge, J. A. Boatz, S. T. Elbert, M. S. Gordon, J. H. Jensen, S. Koseki, N. Matsunaga, K. A. Nguyen, S. Su, T. L. Windus, M. Dupuis, J. A. Montgomery, *J. Comput. Chem.* **1993**, *14*, 1347–1363.
[41] O. V. Dolomanov, L. J. Bourhis, R. J. Gildea, J. A. K. Howard, H. Puschmann, *J. Appl. Crystallogr.* **2009**, *42*, 339–341.
[42] G. M. Sheldrick, *Acta Crystallogr., Sect. A* **2008**, *64*, 112–122.
Received: January 14, 2014
Published Online: March 20, 2014

